Electronic Supplementary Material (ESI) for CrystEngComm.

Supporting information

Content

1. Chemicals

Table S1 All chemicals were used without further purification.

chemicals	producer
4-Bromoacetophenone	ABCR
Chloroform	Wall
Diethylether	Roth
Ethanol	Roth
Hydrochloric acid 38 %	BASF
1,3-*Iso*propylbenzene	Aldrich
$Mg(SO_4)$	Merck
Methanol	BASF
$Na_2CO_3 \cdot 10H_2O$	Grüssing
NaCl	Merck
$NiCl_2 \cdot 6H_2O$	Merck
NaOH	Grüssing
Thionylchlorid	Merck
Triethylphosphit	Fluka
$Zn(NO_3)_2 \cdot 6H_2O$	Merck

2. Analytical methods

Elemental analysis. Carbon, hydrogen and nitrogen contents were determined by elemental analysis by a EuroEA3000, referenced to Sulfanilamide.

Thermogravimetric analysis. Thermogravimetric measurements were performed under a stream of air (75 mL/min) using a Netsch STA-409CD instrument running from room temperature to 900 °C with a heating rate of 4 K/min.

Nuclear magnetic resonance spectroscopy. ^{1}H-NMR and ^{31}P-NMR spectra were recorded at a Bruker DRX 500 spectrometer. The chemical shift (δ) values are reported in ppm, referenced to tetramethylsilane and phosphoric acid, respectively. The coupling constants (J) are given in Hz. The abbreviations are as follows: s singlet, d doublet, dd doublet of a doublet, t triplet, m multiplet.

Scanning Electron Microscopy. SEM images and EDX measurements were performed with a Philips ESEM XL 30 instrument.

Sorption measurements. 20-40 mg CAU-25 were activated under vacuum for 6 hours at 150 °C. N_2, CO_2 and water sorption measurements were carried out with a Belsorpmax (Bel Japan Inc.).

The IR spectra were recorded on a Bruker ALPHA-P FTIR spectrometer in the spectral range 4000–400 cm^{-1}.

Powder X-ray Diffraction. The PXRD patterns were measured with $CuK_{\alpha1}$ radiation on a Stoe Stadi P diffractometer in transmission geometry, equipped with a CCD detector.

Single Crystal Diffraction. Single crystal X-ray diffraction data were collected on a Nonius Kappa-CCD diffractometer at 173 K using a vertically mounted graphite crystal monocromator, a 95mm CCD camera detector and MoK_α radiation. Computing data collection was done with Collect (Bruker AXS BV, 1997-2004), the data reduction with HKL Denzo and Scalepack [a]. The data were analysed by XPREP[b], and the structure was solved with SHELXS and refined with SHELXL.[c]

[a] Z. Otwinowski and W. Minor, Academic Press (New York), Macromolecular Crystallography, part A, Methods in Enzymology, 1997, **276**, 307.

[b] XPREP version 5.1, Bruker Analytical X-ray Systems, Madison, Wisconsin, USA, 1997.

[c] G.M. Sheldrick, Acta Crystallogr. 2008, **A64**, 112.

4. Porous Metal Phosphonates

Lists of crystalline porous metal phosphonates, whose porosity was proven by gas sorption measurements. Porous compounds in which non-phosphonate molecules were used as a spacer in-between the metal phosphonate layers to generate porosity are excluded.

Table S2a Porous metal methylphosphonates.

Formula sum	Name of organic molecules	
β-$[Al_2(CH_3PO_3)_3]$	Methylphosphonic acid	K. Maeda, Y. Kiyozumi, F. Mizukami, *Angew. Chem. Int. Ed.* 1994, **33**, 2335.
α-$[Al_2(CH_3PO_3)_3]$	Methylphosphonic acid	K. Maeda, J. Akimoto, Y. Kiyozumi, F. Mizukami, *Angew. Chem. Int. Ed.* 1995, **34**, 1199.

Table S2b Porous metal phosphonates, where an additional functional group is added to the linker molecule.

Formula sum	Name of organic molecules	
$[M_2(H_2O)_2(L1)]\cdot xH_2O$, M= Mg, Mn, Fe, Co, Ni	H_4L1= N,N'-piperazinebis (methylenephosphonic acid)	J. A. Groves, S. R. Miller, S. J. Warrender, C. Mellot-Draznieks, P. Lightfoot, P. A. Wright, *Chem. Commun.* 2006, 3305. M. T. Wharmby, G. M. Pearce, J. P. S. Mowat, J. M. Griffin, S. E. Ashbrook, P. A. Wright, L.-H. Schilling, A. Lieb, N. Stock, S. Chavan, S. Bordiga, E. Garcia, G. D. Pirngruber, M. Vreeke, L. Gora, *Micro. Meso. Mater.* 2012, **157**, 3.
$[TiO(H_2L1)]\cdot nH_2O$ (n ~ 4.5)), $[AlOH(H_2L1)]\cdot nH_2O$ (n ~ 3))	H_4L1= N,N'-piperazinebis(methylenephosphonic acid)	C. Serre, J. A. Groves, P. Lightfoot, A. M. Z. Slawin, P. A. Wright, N. Stock, T. Bein, M. Haouas, F. Taulelle, G. Férey, *Chem. Mater.* 2006, **18**, 1451.

$[Ln(H_2L2)_3]\cdot 2H_2O$, Ln= Tb, Dy, Eu, Gd	H_3L2= N-(phosphonomethyl) proline	Q. Yue, J. Yang, G.-H. Li, G.-D. Li, J.-S. Chen, *Inorg. Chem.* 2006, **45**, 4431.
$[M_2(H_2L3)_3]\cdot 7H_2O$, M= Gd-Yb, Y, Sc	H_4L3= N,N′-2-methylpiperazinebis(methylene phosphonic acid)	M. T. Wharmby, S. R. Miller, J. A. Groves, I. Margiolaki, S. E. Ashbrook, P. A. Wright, *Dalton Trans.* 2010, **39**, 6389.
$[M_2(H_2O)_2L4]\cdot 11H_2O$; M= Ni, Co	H_4L4= N, N'-4,4'-bipiperidinebis-(methylenephosphonic acid)	M. T. Wharmby, J. P. S. Mowat, S. P. Thompson, P. A. Wright, *J. Am. Chem. Soc.* 2011, **133**, 1266.
$[La(L5)_4(H_2O)_6]Cl\cdot xH_2O$	H_2L5 = 4-(4H-1,2,4-triazol-4-yl)phenyl phosphonic acid	S. Begum, Z. Wang, A. Donnadio, F. Costantino, M. Casciola, R. Valiullin, C. Chmelik, M. Bertmer, J. Kärger, J. Haase, H. Krautscheid, *Chem.--Eur. J.* 2014, **20**, 8862.
$[Co_4(L5)_3(OH)(H_2O)_3](SO_4)_{0.5}\cdot xH_2O$	H_2L5 = 4-(4H-1,2,4-triazol-4-yl)phenyl phosphonic acid	S. Begum, S. Horike, S. Kitagawa, H. Krautscheid, *Dalton Trans.* 2015, **44**, 18727.

Table S2c Porous metal phosphonate monoesters.

Formula sum	Name of organic molecules	
[CuL6]	H_2L6 = 1,4-benzenediphosphonate *bis*(mono methyl ester)	S. S. Iremonger, J. Liang, R. Vaidhyanathan, I. Martens, G. K. H. Shimizu, T. D. Daff, M. Z. Aghaji, S. Yeganegi, T. K. Woo, *J. Am. Chem. Soc.* 2011, **133**, 20048.
[ZnL7]	H_2L7 = 1,4-benzenediphosphonate *bis*(mono ethyl ester)	S. S. Iremonger, J. Liang, R. Vaidhyanathan, G. K. H. Shimizu, *Chem. Commun.* 2011, **47**, 4430.
$[BaH_2L8]$	H_4L8= tetraethyl-1,3,6,8-pyrenetetraphosphonic acid	J. M. Taylor, R. Vaidhyanathan, S. S. Iremonger, G. K. H. Shimizu, *J. Am. Chem. Soc.* 2012, **134**, 14338.

Table S2d Porous metal phosphonates, where the formation of a dense layered structure motif is disrupted by adjustment of the geometry of the linker molecule.

Formula sum	Name of organic molecules	
$[Cu_3(H_3L9)(OH)(H_2O)_3]\cdot H_2O\cdot CH_3OH$	H_8L9= 1,3,5,7-*tetrakis*(4-phenylphosphonic acid)-adamantane	J. M. Taylor, A. H. Mahmoudkhani, G. K. H. Shimizu, *Angew. Chem. Int. Ed.* 2007, **46**, 795.
$[Sr_2(H_2PPB)(CH_3OH)(H_2O)_4]$	H_6PPB = 1,3,5-*tris*-(4-phosphonophenyl)benzene	R. Vaidhyanathan, A. H. Mahmoudkhani, G. K. H. Shimizu, *Can. J. Chem.* 2009, **87**, 247.
$[Sn(H_2PPB)]\cdot 4.5\ H_2O$	H_6PPB = 1,3,5-*tris*-(4-phosphonophenyl)benzene	R. K. Mah, M. W. Lui, G. K. H. Shimizu, *Inorg. Chem.* 2013, **52**, 7311.
$[Zr(H_4TTBMP)_2]\cdot 10H_2O$	H_6TTBMP = 2,4,6-*tris*(4-(phosphonomethyl)phenyl)-1,3,5-triazine	M. Taddei, F. Costantino, F. Marmottini, A. Comotti, P. Sozzani, R. Vivani, *Chem. Commun.* 2014, **50**, 14831.
$[Al(H_3TMBTMP)(H_2O)]$	$H_6TMBTMP$= (2,4,6-trimethylbenzene-1,3,5-triyl)*tris*(methylene) triphosphonic acid	S.-F. Tang, J.-J. Cai, L.-J. Li, X.-X. Lv, C. Wang, X.-B. Zhao, *Dalton Trans.* 2014, **43**, 5970.
$[Cu_3(PPT)(H_2O)_3]\cdot 10H_2O$	H_6PPT = 2,4,6-*tri*-(phenylene-4-phosphonic acid)-*s*-triazine	N. Hermer, N. Stock, *Dalton Trans.* 2015, **44**, 3720.
$[Zr(H_2PPB)]\cdot 7H_2O$	H_6PPB = 1,3,5-*tris*-(4-phosphonophenyl)benzene	R. K. Mah, B. S. Gelfand, J. M. Taylor, G. K. H. Shimizu, *Inorganic Chemistry Frontiers* 2015, **2**, 273.

4. Metal phosphonates with H_6PPB

Table S3 Metal phosphonates with H_6PPB.

Forula sum	Sorption behavior	
$[Sr_2(H_2PPB)(CH_3OH)(H_2O)_4]$	Porous against CO_2, and H_2O	R. Vaidhyanathan, A. H. Mahmoudkhani, G. K. H. Shimizu, *Can. J. Chem.* 2009, **87**, 247.
$[V_3O_3(OH)(H_3PPB)_2]\cdot 7\ H_2O$	Not tested	W. Ouellette, G. Wang, H. Liu, G. T. Yee, C. J. O'Connor, J. Zubieta, *Inorg. Chem.* 2009, **48**, 953.
$[Sn(H_2PPB)]\cdot 4.5\ H_2O$	Porous against N_2 and CO_2	R. K. Mah, M. W. Lui, G. K. H. Shimizu, *Inorg. Chem.* 2013, **52**, 7311.
$[Zr_3(H_3PPB)_4]\cdot 15\ H_2O$	Not porous against N_2	M. Taddei, F. Costantino, R. Vivani, S. Sabatini, S.-H. Lim, S. M. Cohen, *Chem. Commun.* 2014, **50**, 5737.
$[Zr(H_2PPB)]\cdot 7H_2O$	Porous against N_2 and CO_2	R. K. Mah, B. S. Gelfand, J. M. Taylor, G. K. H. Shimizu, *Inorganic Chemistry Frontiers* 2015, **2**, 273.

5. Synthesis of tris(4-bromophenyl)benzene

50 g (0.25 mol) of 4-bromoacetophenone were dissolved in 200 mL ethanol. 31 mL (0.42 mol) of thionylchloride were added slowly. The reaction mixture was heated to 60 °C for 1 h and 100 mL of saturated sodium carbonate solution was added. The solid was filtered, and washed with 50 mL water, ethanol and diethyl ether, respectively.

32.4 g (59.8 mmol, 72 %, yield reported in literature: 72%[9]) of a yellow solid were recovered.

^{1}H-NMR (200 MHz, $CDCl_3$, 300 K, TMS): δ = 7.68 (s, 3 H, H-1), 7.57 (m, 12 H, H-2, H-3) ppm.

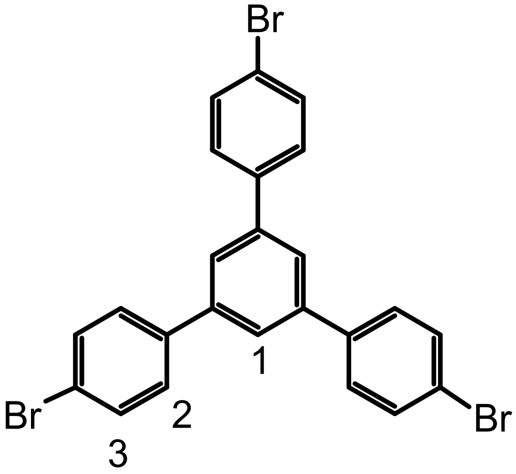

6. Synthesis of 1,3,5-tris-(4-diethylphosphonophenyl)benzene

$NiCl_2 \cdot 6H_2O$ was dried for 5 h in a N_2 stream at 150 °C. 20.0 g (36.8 mmol) Tris(4-bromophenyl)benzene and 5.0 g (38.6 mmol) $NiCl_2$ were suspended in 250 mL 1,3-isopropylbenzene and heated to 170 °C. 40 mL (0.20 mol) triethylphosphite were added slowly. The mixture was held at 170°C for 20 h. The solvent was removed under reduced pressure and 200 mL of water and chloroform were added, respectively. The mixture was heated to 60 °C for 30 min, the aqueous and the organic phase were separated and the aqueous phase was extracted with chloroform (4 times 80 mL). The organic phase was dried with $Mg(SO_4)$, which was filtered off and the solvent was removed under reduced pressure. The solid was recrystallized from ethanol.

22.0 g (31 mmol, 84%, yield reported in literature 84%[5]) of a pale yellow powder were recovered.

^{1}H-NMR (200 MHz, $CDCl_3$, 300 K, TMS): δ = 7.87 (m, 6 H, H-3), 7.76 (s, 3 H, H-1), 7.71 (m, 6-H, H-2), 4.09 (q, 12 H, ^3J = 7.0 Hz, CH_2), 1.29 (t, 18 H, ^3J = 7.0 Hz, CH_3) ppm.

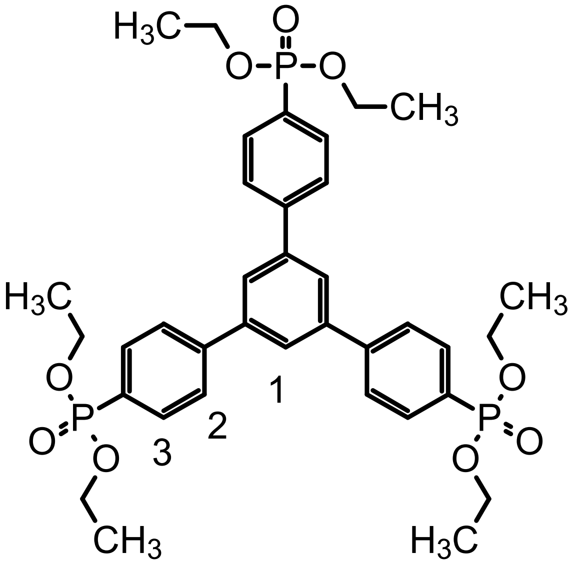

7. Synthesis of 1,3,5-tris-(4-phosphonophenyl)benzene (H_6PPB)

200 mL concentrated HCl were added to 22.8 g (32.0 mmol) 1,3,5-tris-(4-diethylphosphonophenyl)benzene. The mixture was heated to reflux for 20 h. The solvent was removed under reduced pressure. The solid was recrystallized from methanol.

15.8 g (28.8 mmol), 90 %, yield reported in literature 90 %[5]) of a colorless powder were recovered.

IR $\tilde{\nu}$ (cm^{-1}) = 2969 (w), 2716 (b), 2283 (b), 1927 (w), 1700 (b), 1597 (m), 1556 (w), 1504 (w), 1477 (w),1447 (w), 1386 (m), 1135 (s), 986 (s), 919 (s), 867 (m), 818 (s), 688 (s), 606 (m), 547 (s), 514 (m), 425 (m).

^{1}H-NMR (200 MHz, DMSO, 300 K, TMS): δ = 7.94 (m, 6 H, H-3). 7.91 (s, 3 H, H-1), 7.86 (m, 6-H, H-2) ppm.

^{31}P-NMR (200 MHz, MeOD, 300 K, H_3PO_4): 16.06 ppm.

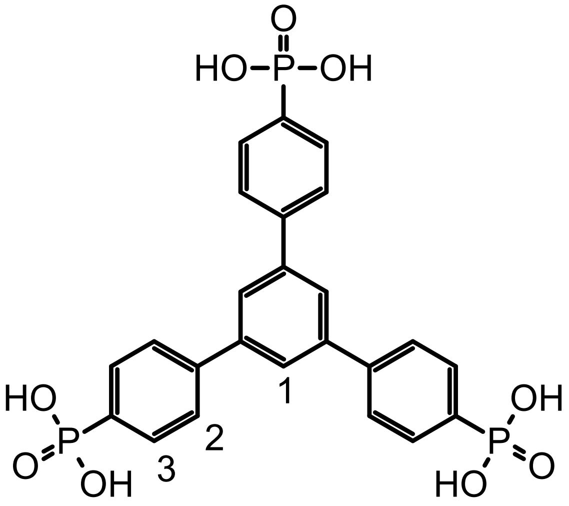

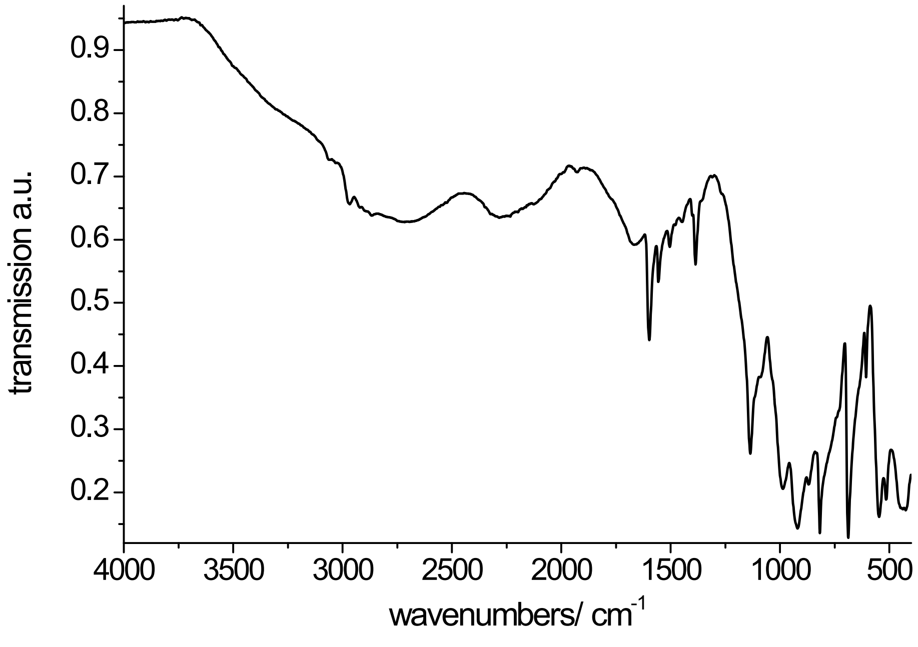

Fig. S1 IR spectrum of 1,3,5-Tris-(4-phosphonophenyl)benzene (H_6PPB).

8. Synthesis of [$Zn_2(H_2PPB)(H_2O)_2$]·x H_2O (CAU-25)

CAU-25 is obtained in a Teflon-lined autoclave (V_{max} = 2 mL) by reaction of a mixture of H_6PPB (30 mg, 55 mmol), aqueous 2 M $Zn(NO_3)_2$ (27.5 µL, 55 mmol), aqueous 2 M NaOH (54.9 µL, 110 mmol), 152 µL deionised water and 366 µL methanol. The reactor was slowly heated to 120 °C within 24 h. The temperature was kept for 24 h and the reactor was subsequently cooled to room temperature within 16 h. The precipitate was filtered of and washed with water and methanol.

17.2 mg (25 mmol, 45 % based on H_6PPB) of a colourless powder were obtained.

Elemental analysis: Calculated for $C_{24}H_{19}P_3O_{10}Zn_2$: C = 41.7 %, H = 2.8 %, Found: C = 42.3 %, H = 3.1 %.

IR $\tilde{\nu}$ (cm^{-1}) = 3486 (w, O-H str.), 3063 (w, C-H str.), 3030 (w, C-H str.), 2953 (w), 2359 (w), 2328 (w), 1650 (w, P-O-H), 1635 (w, O-H def.), 1598 (m, C=C str.), 1558 (w, Phenyl), 1506 (w, Phenyl), 1385 (m, C=C str.), 1139 (s, P=O), 1070 (m), 1042 (s), 1017 (m), 939 (s, P-O), 883 (m), 820 (s, Phenyl C-H), 796 (w), 738 (w), 730 (w), 695 (s, Phenyl C-H), 641 (w), 615 (w), 574 (s), 553 (s), 534 (w), 491 (m), 453 (w), 433(w), 413 (w), 389 (m).

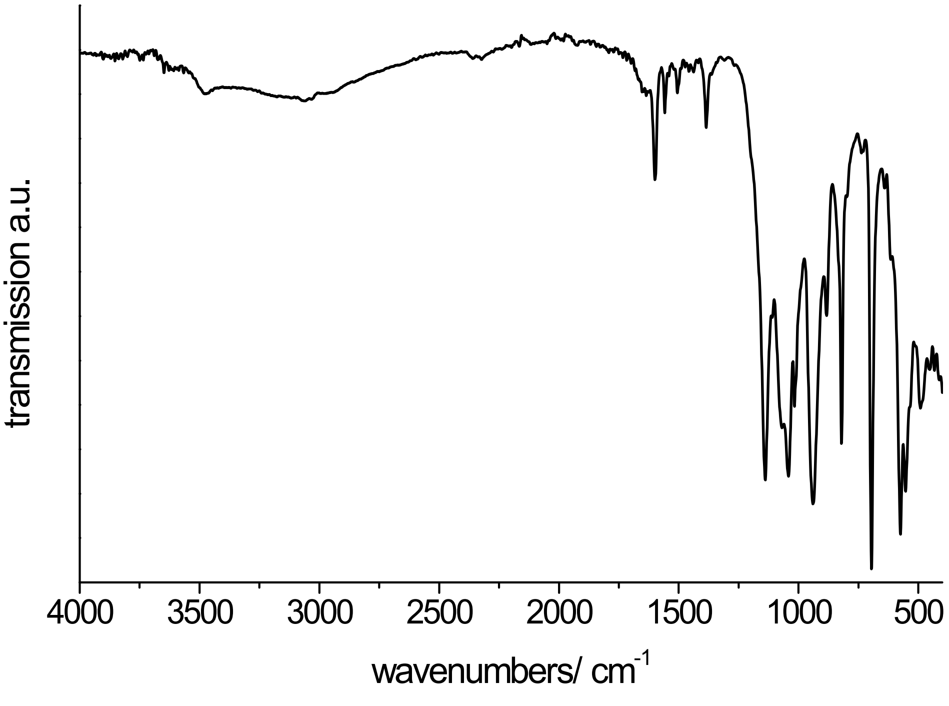

Fig. S2 IR spectrum of [$Zn_2(H_2PPB)(H_2O)_2$]·x H_2O.

9. Crystallisation diagram of the system $Zn^{2+}/H_6PPB/NaOH$ and PXRD patterns of the products

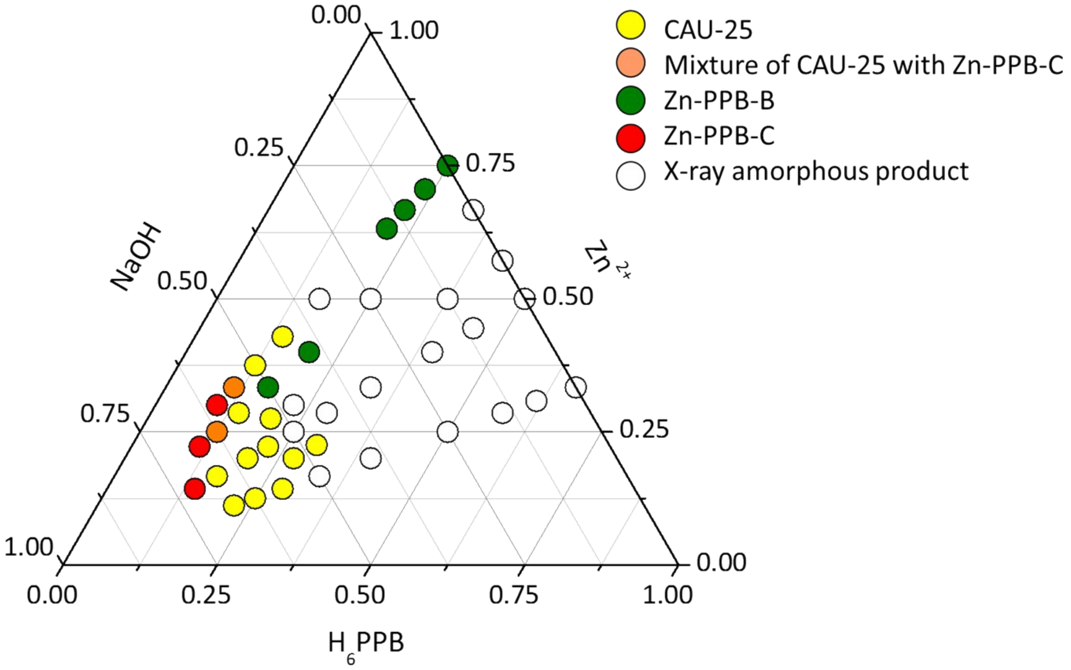

Fig. S3 Crystallisation diagram of the system $Zn^{2+}/H_6PPB/NaOH$. Each point in the diagram corresponds to a distinct molar ratio of the three starting materials.

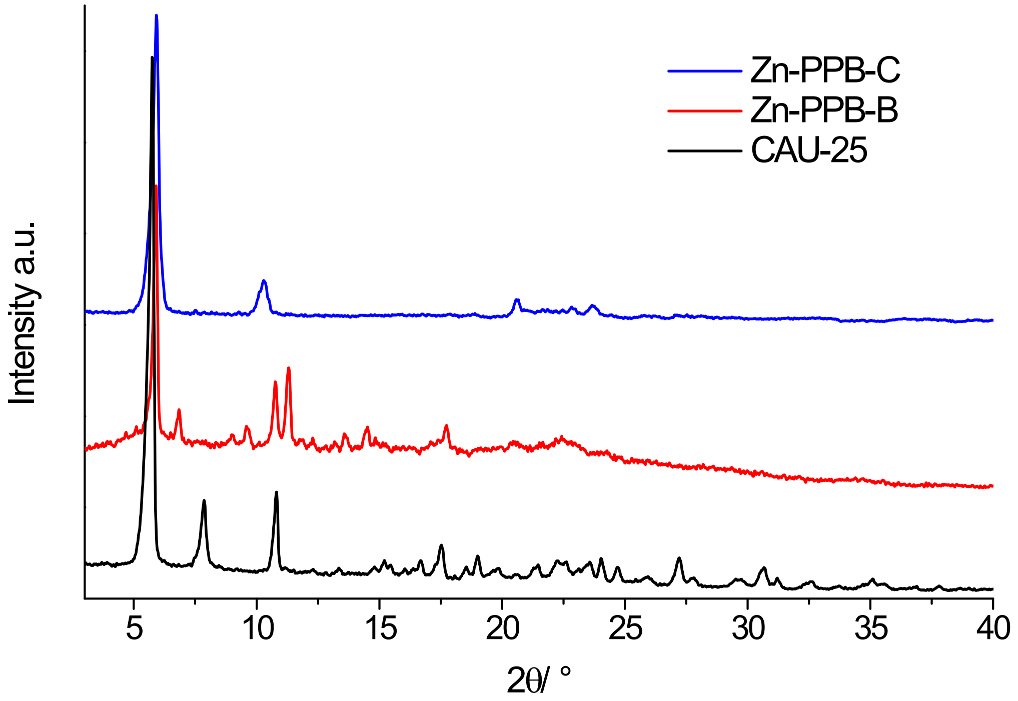

Fig. S4 X-ray powder diffraction patterns of the different products obtained by varying the molar ratios in the system $Zn^{2+}/H_6PPB/NaOH$. The two crystalline products (called Zn-PPB-B and Zn-PPB-C) of low long range order were not further characterized.

Table S4 Investigated ratios and amount of chemicals used for the reactions which the crystallization diagram is based on (Fig. S3). H_6PPB was used as 0.3 M solution in methanol, $Zn(NO_3)_2 \cdot 6H_2O$ and NaOH were used as 2 M aqueous solution. H_6PPB was added first into the autoclaves, afterwards water, Zn^{2+} solution and NaOH solution. The reactor was sealed and slowly heated to 120 °C within 24 h. The temperature was kept for 24 h and the reactor was subsequently cooled to room temperature within 16 h. The precipitate was filtered of and washed with water and methanol.

Molar ratio			Amount of solution added				product
H_6PPB	Zn^{2+}	NaOH	H_6PPB [µL]	H_2O [µL]	$Zn(NO_3)_2$ [µL]	NaOH [µL]	
1	1	0	61.0	130	9.2	0.0	X-ray amorphous
1	1	0.25	61.0	125	9.2	4.6	X-ray amorphous
1	1	0.5	61.0	121	9.2	9.2	X-ray amorphous
1	1	1	61.0	112	9.2	18.3	X-ray amorphous
1	1	1.5	61.0	102	9.2	27.5	X-ray amorphous
1	1	2	61.0	93	9.2	36.6	X-ray amorphous
1	1	2.5	61.0	84	9.2	45.8	CAU-25
1	1	3	61.0	75	9.2	54.9	CAU-25
1	1	4	61.0	57	9.2	73.2	CAU-25
1	1	5	61.0	38	9.2	91.5	Zn-PPB-C
1	2	1	61.0	102	18.3	18.3	Zn-PPB-B
1	2	0	61.0	121	18.3	0.0	X-ray amorphous
1	2	1	61.0	102	18.3	18.3	X-ray amorphous
1	2	2	61.0	84	18.3		Zn-PPB-B
1	2	3	61.0	66	18.3	54.9	Zn-PPB-B
1	2	4	61.0	47	18.3	73.2	CAU-25
1	2	5	61.0	29	18.3	91.5	CAU-25 and Zn-PPB-C
1	2	6	61.0	11	18.3	109.8	Zn-PPB-C

1	0,5	0	61.0	134	4.6	0.0	X-ray amorphous
1	0,5	0,13	61.0	132	4.6	2.3	X-ray amorphous
1	0,5	0,25	61.0	130	4.6	4.6	X-ray amorphous
1	0,5	0,5	61.0	125	4.6	9.2	X-ray amorphous
1	0,5	1	61.0	116	4.6	18.3	X-ray amorphous
1	0,5	1,5	61.0	107	4.6	27.5	X-ray amorphous
1	0,5	2	61.0	98	4.6	36.6	CAU-25
1	0,5	2,5	61.0	89	4.6	45.8	CAU-25
1	0,5	3	61.0	79	4.6	54.9	CAU-25
1	3	0	61.0	112	27.5	0.0	Zn-PPB-B
1	3	0.25	61.0	107	27.5	4.6	Zn-PPB-B
1	3	0.5	61.0	102	27.5	9.2	Zn-PPB-B
1	3	0.75	61.0	98	27.5	13.7	Zn-PPB-B
1	3	2	61.0	75	27.5	36.6	X-ray amorphous
1	3	3	61.0	57	27.5	54.9	CAU-25
1	3	4	61.0	38	27.5	73.2	CAU-25
1	3	5	61.0	20	27.5	91.5	Zn-PPB-C and CAU-25
1	3	6	61.0	2	27.5	109.8	Zn-PPB-C
1	0,73	1,91	61.0	97	6.7	34.9	CAU-25
1	0,75	1,58	61.0	103	6.9	29.0	CAU-25
1	1,33	2,11	61.0	88	12.2	38.6	X-ray amorphous
1	1,38	2,63	61.0	78	12.6	48.1	CAU-25
1	1,33	0	61.0	127	12.2	0.0	X-ray amorphous
1	1,33	0,33	61.0	121	12.2	6.1	X-ray amorphous

10. Structural data of $[Zn_2(H_2PPB)(H_2O)_2]\cdot x\ H_2O$

```
data_
_chemical_name_mineral [Zn2(H2PPB)(H2O)2]·x H2O
_cell_length_a  44.6733(34)
_cell_length_b  16.31097(83)
_cell_length_c  8.29666(30)
_cell_angle_alpha 90
_cell_angle_beta  95.3001(77)
_cell_angle_gamma 90
_cell_volume 6019.64(59)
_symmetry_space_group_name_H-M C12/c1
loop_
_symmetry_equiv_pos_as_xyz
        '-x, -y, -z'
        '-x, y, -z+1/2'
        'x, -y, z+1/2'
        'x, y, z'
        '-x+1/2, -y+1/2, -z'
        '-x+1/2, y+1/2, -z+1/2'
        'x+1/2, -y+1/2, z+1/2'
        'x+1/2, y+1/2, z'
loop_
_atom_site_label
_atom_site_type_symbol
_atom_site_symmetry_multiplicity
_atom_site_fract_x
_atom_site_fract_y
_atom_site_fract_z
_atom_site_occupancy
_atom_site_B_iso_or_equiv
Zn1 Zn   0 0.15619(31) 0.01118(77) 0.4590(18) 1 0.50(29)
Zn2 Zn   0 0.07815(30) 0.00988(81) 0.4331(14) 1 0.50(29)
P1 P   0 0.11488(40) -0.0843(11) 0.2214(23) 1 0.50(29)
O1 O   0 0.11697(74) -0.0315(23) 0.3770(33) 1 0.50(29)
O2 O   0 0.08374(64) -0.0729(28) 0.1334(32) 1 0.50(29)
O3 O   0 0.14242(68) -0.0846(24) 0.1267(27) 1 0.50(29)
P2 P   0 0.19997(38) -0.1119(11) 0.6936(24) 1 0.50(29)
O4 O   0 0.18718(97) -0.0684(23) 0.5347(43) 1 0.50(29)
O5 O   0 0.1906(13) -0.2006(16) 0.6579(50) 1 0.50(29)
O6 O   0 0.17850(90) -0.0873(28) 0.8213(42) 1 0.50(29)
P3 P   0 0.04928(46) -0.1230(10) 0.6640(23) 1 0.50(29)
O7 O   0 0.05927(71) -0.0885(17) 0.5048(32) 1 0.50(29)
O8 O   0 0.01886(67) -0.1671(21) 0.6175(57) 1 0.50(29)
O9 O   0 0.04555(71) -0.0598(22) 0.7953(33) 1 0.50(29)
```

```
C11 C   0 0.3352917 0.0426195 1.023861 1 8.0(10)
C12 C   0 0.3438865 -0.1022635 1.048962 1 8.0(10)
C13 C   0 0.3249362 -0.03701185 0.999212 1 8.0(10)
C14 C   0 0.3723926 -0.08781463 1.128663 1 8.0(10)
C15 C   0 0.3818617 -0.006936686 1.162019 1 8.0(10)
C16 C   0 0.3628715 0.05869471 1.112307 1 8.0(10)
C21 C   0 0.3695041 0.144151 1.161598 1 8.0(10)
C22 C   0 0.3785284 0.3107145 1.228127 1 8.0(10)
C23 C   0 0.3987297 0.1769481 1.171368 1 8.0(10)
C24 C   0 0.4032916 0.2601812 1.207602 1 8.0(10)
C25 C   0 0.3497114 0.2775541 1.22074 1 8.0(10)
C26 C   0 0.3453848 0.1950948 1.193442 1 8.0(10)
C31 C   0 0.2368616 -0.0886061 0.7681193 1 8.0(10)
C32 C   0 0.2801709 0.0007353454 0.806778 1 8.0(10)
C33 C   0 0.2519942 -0.01782905 0.7285882 1 8.0(10)
C34 C   0 0.277934 -0.121797 0.9695041 1 8.0(10)
C35 C   0 0.2496795 -0.1399376 0.8909293 1 8.0(10)
C36 C   0 0.2939104 -0.05132884 0.9277322 1 8.0(10)
C41 C   0 0.3913628 -0.158326 1.181393 1 8.0(10)
C42 C   0 0.4261565 -0.296507 1.271338 1 8.0(10)
C43 C   0 0.421334 -0.1623627 1.145249 1 8.0(10)
C44 C   0 0.3788589 -0.2244142 1.260345 1 8.0(10)
C45 C   0 0.396073 -0.293435 1.303816 1 8.0(10)
C46 C   0 0.4385881 -0.2315736 1.188719 1 8.0(10)
Ow1 O   0 0.5 0.4091(49) 0.25 1.000(67) 0.50(29)
```

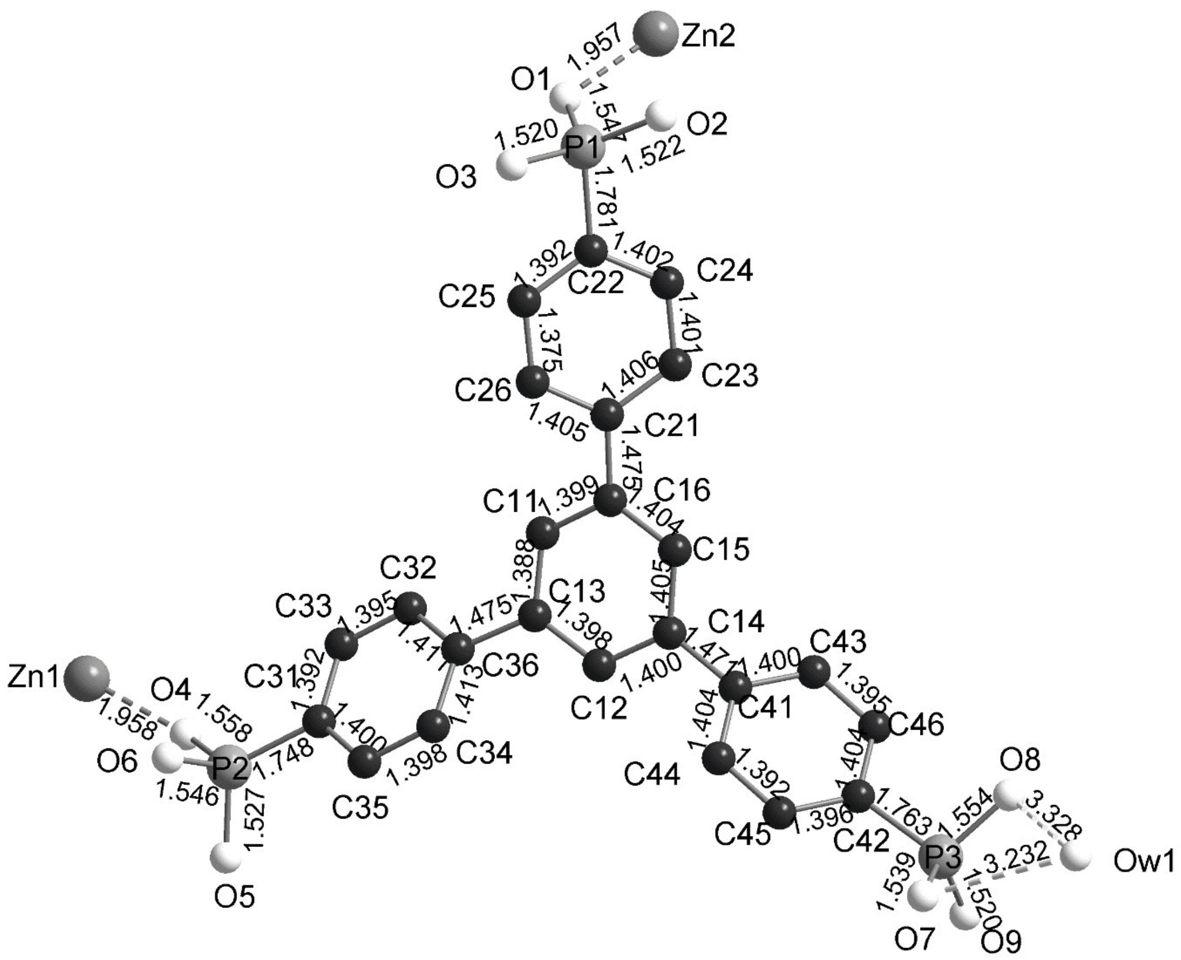

Fig. S5 The asymmetric unit of CAU-25.

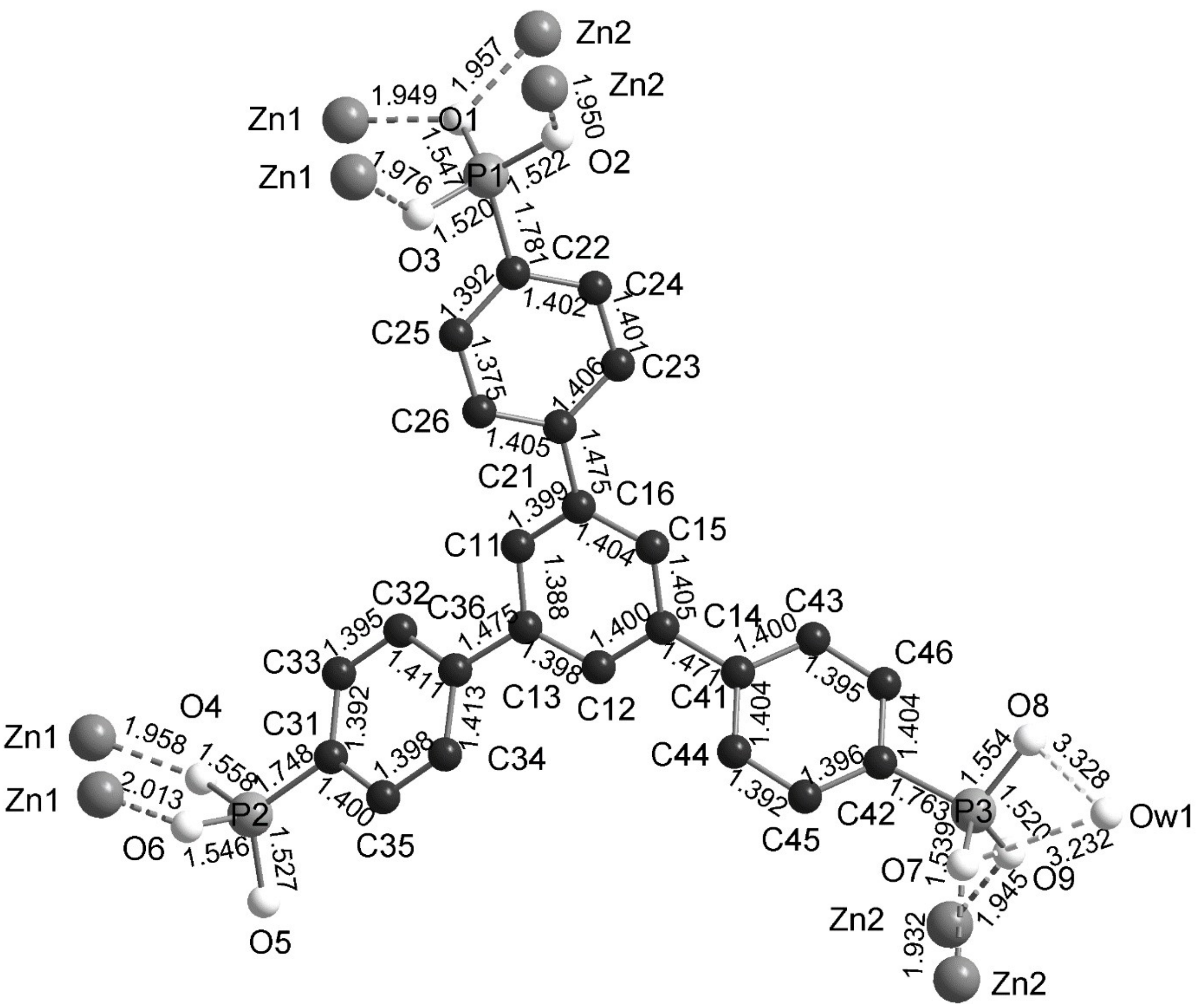

Fig. S6 Coordination environment of H_2PPB molecule in CAU-25 structure.

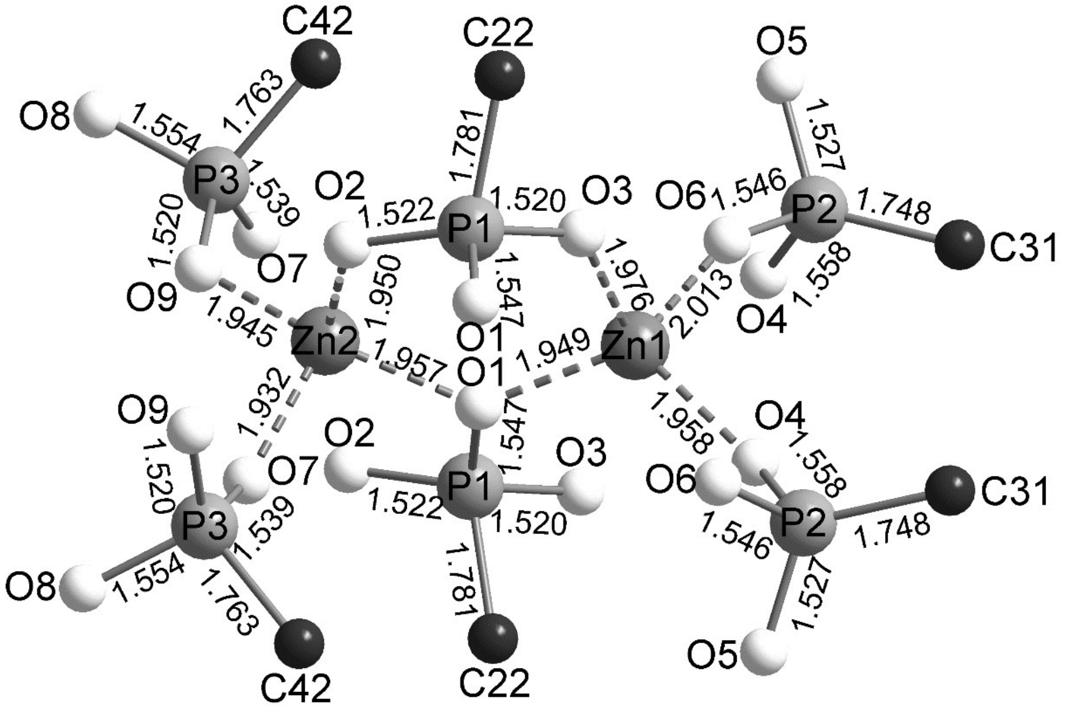

Fig. S7 Coordination environment of Zn^{2+} ions in the CAU-25 structure.

Table S5 Selected bond lengths of CAU-25. Standard deviation is only given for freely refined atoms, the carbon backbone of the linker molecule was refined as rigid body.

Atom 1	Atom 2	Bond lengh/ Å	Atom 1	Atom 2	Bond lengh/ Å
Zn1	O1	1.948(4)	C12	C14	1.399
	O4	1.959(4)	C13	C36	1.398
	O3	1.976(3)	C14	C15	1.405
	O6	2.012(4)		C41	1.471
Zn2	O7	1.933(3)	C15	C16	1.405
	O9	1.945(3)	C16	C21	1.475
	O2	1.950(4)	C21	C26	1.405
	O1	1.957(4)		C23	1.406
P1	O3	1.520(4)	C22	C25	1.392
	O2	1.522(3)		C24	1.402
	O1	1.548(4)	C23	C24	1.401
	C22	1.781(3)	C25	C26	1.375
O2	Zn2	1.950(4)	C31	C33	1.392
	Zn2	2.861(3)		C35	1.399
P2	O5	1.529(3)	C32	C33	1.395
	O6	1.546(4)		C36	1.411
	O4	1.558(4)	C33	C32	1.395
	C31	1.747(2)	C34	C35	1.398
P3	O9	1.520(4)		C36	1.413
	O7	1.539(4)	C41	C43	1.400
	O8	1.555(4)		C44	1.404
	C42	1.763(3)	C42	C45	1.396
C11	C13	1.386		C46	1.404
	C16	1.399	C43	C46	1.395
C12	C13	1.398	C44	C45	1.392

Table S6 Selected O···O distances of CAU-25.

Atom 1	Atom 2	Bond lengh/ Å
Ow1	O9	3.191(7)
	O7	3.2322(3)
	O8	3.3282(5)
O8	O8	2.891(9)

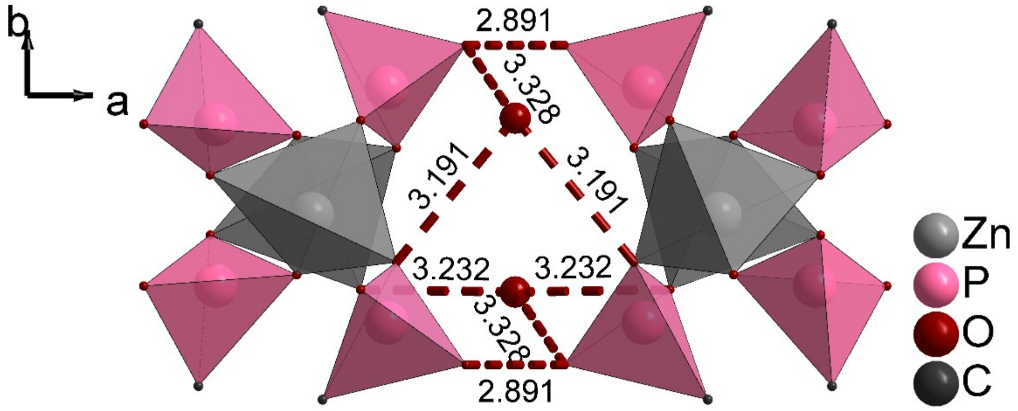

Fig S8 Possible hydrogen bonding based on O···O distances which connects the double-layers via P-O-H···O-P and P-O···H_2O···O-P hydrogen bonds.

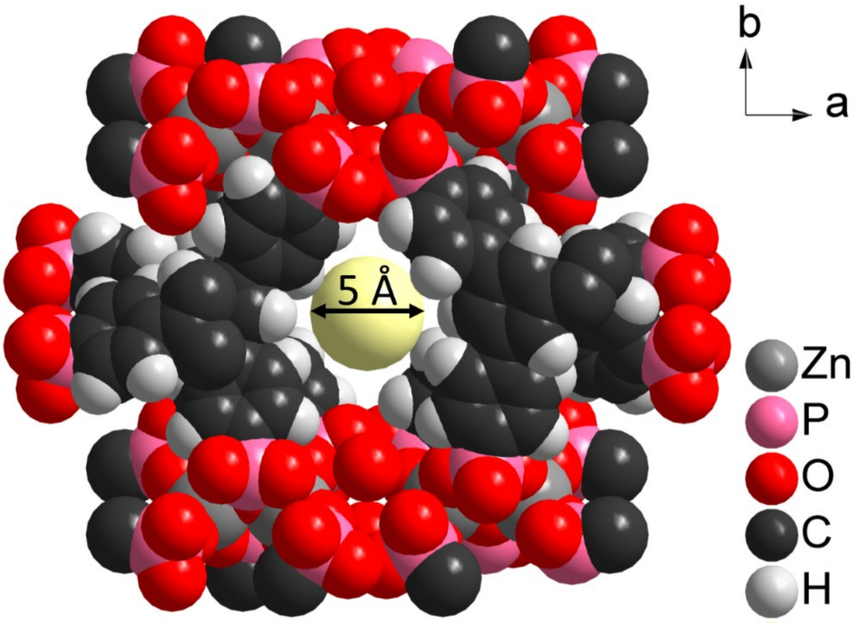

Fig S9 Space filling model of one pore of CAU-25, view along the *c*-axis. To determine a realistic pore diameter protons were generated by the routine implemented in Materials Studio.[13] A sphere of 5 Å in diameter is added to demonstrate the approximate pore size.

11. Thermogravimetric measurement

Table S7 Observed and measured weight changes during the thermogravimetric measurement of CAU-25.

Temperature	Change of weight	Reaction, calculated weight loss
To 100 °C	-4 %	Loss of weakly bound solvent molecules, 1.7 H_2O per formula sum (4 %)
100 °C to 400 °C	-5 %	Loss of strongly bound water molecules, 2 H_2O per formula sum (5 %)
400 °C to 800 °C	-41 %	Oxidation of organic part ($C_{24}H_{17}$) (41 %)

12. PXRD after sorption analysis

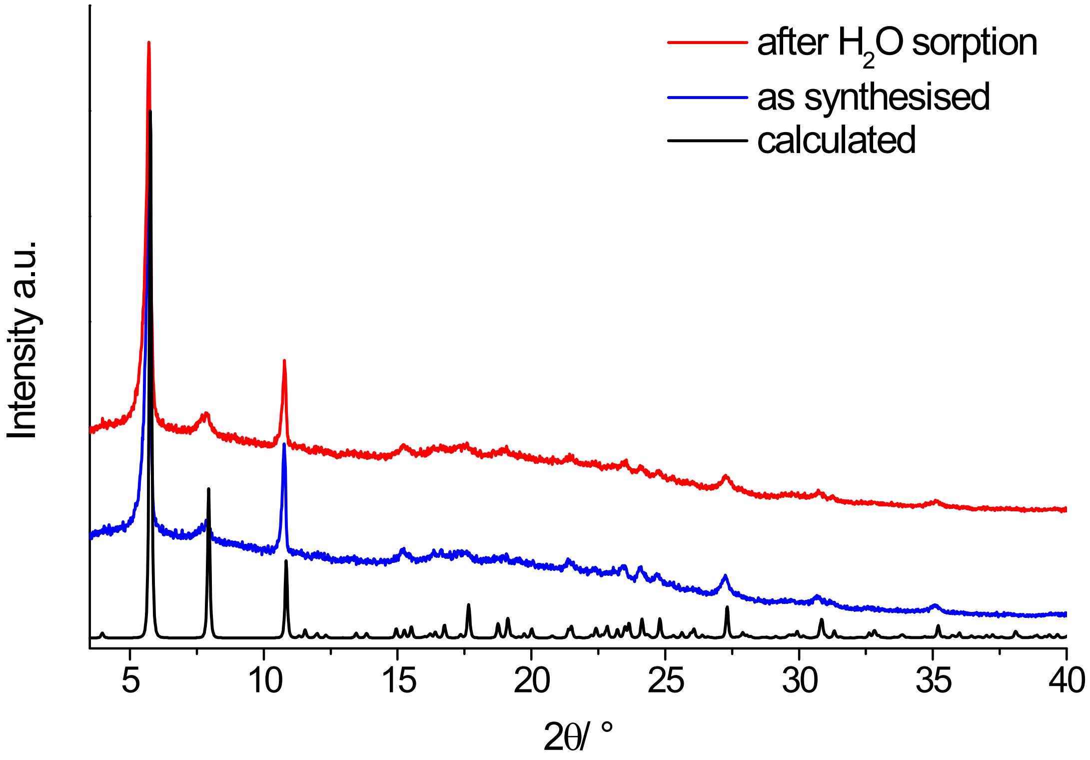

Fig. S10 Comparison of the PXRD patterns of as-synthesized compound (blue curve) and after the H_2O sorption measurements (red curve) with a simulated PXRD pattern (black curve).